Research Square

Preprints are preliminary reports that have not undergone peer review.
They should not be considered conclusive, used to inform clinical practice,
or referenced by the media as validated information.

Morphological and Morphometric Characterization of the Submandibular Fossa Using Cone-Beam Computed Tomography

Jessica Helena Vieira Granato
State University of Ponta Grossa
Fabio Brasil Oliveira
State University of Ponta Grossa
Kellen Rutes Donato
State University of Ponta Grossa
Leonardo Christiaan Welling
State University of Ponta Grossa
Amanda Regina Fischborn
State University of Ponta Grossa
Gilson Cesar Nobre Franco
State University of Ponta Grossa
Marcela Claudino
marcelaclaudino@hotmail.com
State University of Ponta Grossa

Research Article

Keywords: Cone-Beam Computed Tomography, Submandibular Gland, Anatomy, Cortical Bone, Oral Surgery

Posted Date: July 1st, 2026

DOI: https://doi.org/10.21203/rs.3.rs-9981422/v1

License: This work is licensed under a Creative Commons Attribution 4.0 International License.
Read Full License

Additional Declarations: No competing interests reported.

Abstract

Purpose

To evaluate the morphology and morphometry of the submandibular fossa (SMF) in the second premolar and second molar regions, assessing differences between sexes, sides, and tooth regions using Cone-Beam Computed Tomography (CBCT).

Methods

This retrospective, descriptive study evaluated CBCT scans of individuals over 18 years old with posterior teeth present up to the second molar. Scans compromising the analysis of the lingual cortex or mandibular canal were excluded. Cross-sectional images were analyzed using CS 3D Suite software. The lingual cortex was classified into types C (convex), P (parallel), and U (concave), and depth, angulation, height, and buccolingual width were measured. Data were analyzed in Jamovi using Welch's ANOVA and chi-square tests, with a significance level of 5%.

Results

Of the 504 regions evaluated, 73% exhibited a lingual concavity, with a predominance of types U-III (29.6%) and U-II (25.2%). The second molar showed deeper concavities and lower available bone height compared to the second premolar ($p < 0.001$). Males presented larger linear dimensions ($p < 0.001$), with no significant differences regarding the shape and depth of the concavity. Bilateral asymmetry was observed in the second molar, with higher values on the right side.

Conclusion

The greater depth of the SMF in the second molar and on the right side indicates higher surgical risk, regardless of sex, reinforcing the critical importance of preoperative planning using CBCT.

1. Introduction

Dental implants are widely recognized as a viable and predictable alternative for the rehabilitation of edentulous ridges and single-tooth replacements, demonstrating high success rates [1, 2, 3]. However, these elevated success rates depend on functional bone availability, which encompasses both quantitative and qualitative aspects [4]. Consequently, a detailed evaluation of the bone architecture is paramount to minimize intra- and postoperative complications [1, 5]. This analysis is also critical to ensure implant stability and longevity [4, 6], given that anatomical limitations of the alveolar cortical bone can impose restrictions on implant positioning and angulation [1–4, 6].

Within this context, several anatomical structures in the posterior region of the mandible must be thoroughly assessed, such as the mandibular canal (MC) and the mental foramen (MF), since damage to these areas can increase the risk of severe hemorrhages [3, 6–8]. In addition to these structures, the submandibular fossa (SMF) constitutes one of the main anatomical variations associated with surgical risk in the posterior mandible [4, 9, 10]. Also known as the submandibular fovea, the SMF is a depression located on the lingual aspect of the mandibular body, on its internal and inferior surface below the mylohyoid line, which accommodates the submandibular gland [3, 10, 11]. The morphology of the lingual cortex can be classified into three main types: C, characterized by a convex surface with no evident concavity; P, which presents a virtually flat surface parallel to the buccal cortical bone; and U, marked by an evident and well-defined concavity [3, 6, 8, 9]. This classification is clinically significant, as morphologies exhibiting pronounced undercuts and reduced bone thickness are associated with a higher risk of lingual cortical perforation during surgical procedures [2, 3].

In a study by Nickenig et al. (2007) [12], 68% of the molar regions exhibited lingual concavities, whereas Alqutaibi et al. (2024) [13] identified a prevalence of up to 62.7% in the second molar region. Furthermore, investigations evaluating implant placement in the posterior mandible report a probability of lingual cortical perforation ranging between 0.8% and 2.0% [6, 7, 12]. Such complications can involve vital vascular structures, including the lingual, submental, and mylohyoid arteries [3, 7, 10, 14, 15]. Studies indicate that most hemorrhagic episodes in the floor of the mouth and sublingual space have an iatrogenic origin [1, 3, 16].

Therefore, performing complementary examinations during the preoperative period is essential for adequate planning, thereby minimizing intra- and postoperative complications [1, 15, 16]. In this regard, a multidisciplinary approach is crucial, integrating the dental surgeon with physicians, pharmacists, and nurses for an integrated evaluation of the patient's systemic and pharmacological history [1, 3]. This integration aims to manage iatrogenic risks and guide emergencies, such as hemorrhages and airway obstruction resulting from lingual cortical perforation, ultimately preserving the patient's life and serving as an essential pillar in the management of these critical cases [1, 3, 6]. This comprehensive evaluation of the posterior mandible for implant installation primarily requires diagnostic imaging.

Although intraoral and extraoral radiographs are widely used [1, 10, 11, 17], these two-dimensional examinations present several disadvantages, such as image superimposition and distortion, which can significantly compromise the evaluation of this region [2, 3, 7]. Cone-beam computed tomography (CBCT) stands out by offering three-dimensional, highly detailed, high-resolution images free of superimposition. CBCT is indicated for identifying buccal and lingual concavities of the mandible [2, 7, 15], and is characterized as an accurate method for anatomical analysis and linear measurements [10, 11, 14, 15]. Numerous studies [3, 9, 14] have demonstrated its superiority over panoramic radiography. Tal et al. [17] reinforced its advantages in assessing bone shape and volume, showcasing its superior performance in evaluating mandibular structures [5, 11, 15].

Although several studies address the buccolingual dimensions and various morphological classifications of the lingual aspect of the mandible, specific data regarding the submandibular fossa remain limited [3, 4]. These investigations focus predominantly on evaluating the depth of the SMF concavity and its relationship with the mandibular canal. However, more specific morphological aspects, such as angulation, height, buccolingual width, and the distinct cortical shapes (C, P, and U), alongside comparisons between tooth regions and bilateral asymmetry (lateralities), remain poorly explored, highlighting the need for more detailed studies [3, 4]. Therefore, the purpose of this study was to evaluate the morphology and morphometry of the submandibular fossa, as well as its prevalence in the mandibular second premolar and second molar regions, identifying variations regarding sex, tooth region, and right and left sides.

2. Objectives

To evaluate the prevalence and the morphological and morphometric characteristics of the lingual concavity in the posterior mandible (second premolar [2PM] and second molar [2M] regions) using CBCT, analyzing anatomical variations between tooth regions, mandibular sides, and sex.

3. Methods

3.1 Study Design and Sample Selection

This retrospective, descriptive study was approved by the Institutional Review Board (Ethics Committee in Research) of the Universidade Estadual de Ponta Grossa (UEPG) under protocol number 69086823.3.0000.0105, in compliance with the CNS Resolution 466/12. The sample was retrieved from a pre-existing database of the LODI Diagnostic Imaging Center, affiliated with UEPG, comprising cone-beam computed tomography (CBCT) scans performed between January 2020 and December 2025. The inclusion criteria were: individuals aged > years, of both sexes, presenting mandibular posterior teeth up to the second molar. Two scans were excluded due to extensive metallic artifacts and lack of clear visualization of the mandibular canal.

Sample size calculation considered the male and female groups, with the depth of the concavity (D) as the primary variable. Employing an effect size of 0.5, a statistical power of 0.8, an estimated standard deviation of 1.0 mm, and a minimum clinically relevant difference of 0.5mm, a minimum sample of 126 examinations was determined, in accordance with previous studies [2, 3, 14].

3.2 CBCT Image Acquisition

omographic images were acquired using an i-CAT Next Generation® device (Imaging Sciences International, Hatfield, PA, USA), operating with a 14-bit grayscale depth and a 0.5 mm focal spot. The acquisition parameters applied to all patients were: X-ray tube voltage of 120 kVp, tube current ranging between 3 and 8 mA, field of view (FOV) of 17 × 23 mm or 16 × 13 mm, voxel size of 0.3 mm and an

acquisition time of 17.8 segundos. Image acquisition was performed by qualified oral and maxillofacial radiologists.

3.3 Image Analysis

Image analyses were executed using the CS 3D Suite software, version 3.10.38 (Carestream Health, Rochester, NY, USA), in an environment with controlled lighting and high-resolution monitors. All examinations were evaluated anonymously. Prior to measurements, the images were reoriented in multiplanar reconstruction (MPR) mode by adjusting the mandibular midline and the axial slice plane parallel to the occlusal plane. Parasagittal cross-sections were generated perpendicular to the mandibular arch, with a slice thickness of 1,0 mm. The evaluations were performed using a standardized zoom of 200% and a precision of 0,01 mm.

Morphological and morphometric analyses were performed bilaterally on the distal aspect of the mandibular second premolar (2PM) and mandibular second molar (2M) regions.

3.4 Morphological Evaluation

The cross-sectional configuration of the lingual cortical bone was classified into three main categories [5, 14] (Figure 1):

· Convex (C): A convex lingual cortex without undercuts, presenting a wider base and a narrower alveolar crest.

· Concave (U): A surface with a pronounced depression (undercut) in the submandibular fossa (SMF), featuring a narrow base and a wider intermediate portion, defining the most prominent point (Point A) on the lingual cortex.

· Flat (P): Parallel buccal and lingual cortical plates, with no evident undercut.

The regions classified as type U were further subdivided according to the depth of the concavity (D) into three subtypes [2, 14] (Figure 2):

- Type I (Shallow): $D < 2.0$ mm;
- Type II (Moderate): $2{,}0 \text{ mm} \leq D \leq 3.0$ mm;
- Type III (Deep): $D > 3.0$ mm.

For linear evaluation, the cross-section showing the greatest depth of the lingual concavity was selected in each region (2PM and 2M). Point A was established as the most prominent lingual point of the crest, and Line X as the horizontal line drawn 2 mm above the roof of the mandibular canal. Point B was defined as the intersection of the lingual cortex with Line X. Line Y connected Point A to Line X for angular measurement (Figure 3).

Seven measurements (in millimeters) were performed in each region [1, 2, 14] (Figures 4 and 5):

1. Available bone height (Va): Vertical distance between the alveolar bone crest and Line X (the line passing 2 mm above the mandibular canal).

2. Height of the concavity (Vc): Vertical distance from the alveolar bone crest to Point A.

3. Vertical position of the concavity (Vb): Vertical distance from the inferior border of the mandible to Point A.

4. Depth of the concavity (D): Horizontal distance between the most prominent point of the lingual aspect (A) and the intersection point of Line Y with the lingual cortex.

5. Superior buccolingual width (WA): Horizontal measurement at the most coronal level, 2mm below the alveolar bone crest.

6. Inferior buccolingual width (WB): Horizontal measurement at the level of Line X (2mm above the mandibular canal).

7. Angle of the concavity (β): Angle formed between Line Y and Line X, tangent to the most prominent point of the concavity.

3.5 Statistical Analysis

Statistical analyses were performed using Jamovi software, version 2.6 (The Jamovi Project, 2024). Data were submitted to descriptive analysis expressed as mean and standard deviation for morphometric (continuous) variables, and as absolute and relative frequencies (percentages) for categorical variables.

The comparison of morphometric means among sexes, tooth regions (2PM and 2M), and mandibular sides was performed using Welch's one-way ANOVA, due to the heterogeneity of variances (heteroscedasticity) observed between groups.

For categorical variables regarding the morphology of the lingual cortex (C, P, U-I, U-II, and U-III classifications), the association with the variables sex, side, and tooth region was evaluated using Pearson's chi-square test. In cases where the expected frequencies were lower than 5, Fisher's exact test was applied. The significance level adopted for all analyses was 5% ($p < 0.05$).

4. Results

The sample consisted of 126 CBCT scans, totaling 504 evaluated tooth regions, corresponding to the right and left sides of the mandibular second premolar (2PM) and mandibular second molar (2M) regions. The sample was equally distributed between sexes, with 252 tooth regions from male subjects and 252 from female subjects.

The distribution analysis of the lingual cortex types showed that, among the entire sample, type U-III was the most prevalent, occurring in 149 evaluated regions (29.6%), as demonstrated in Graph 1. This was followed by type U-II with 127 cases (25.2%), also demonstrating a high frequency. Subtype U-I appeared in 92 regions (18.3%). Type P cortices represented 17.9% of the sample, while type C was the least frequent, occurring in 9.1% of the regions. These results indicate that approximately 73% of the evaluated regions exhibited some degree of lingual concavity, with more than half corresponding to moderate or deep concavities (U-II and U-III).

The distribution of the morphological types of the lingual cortex showed statistically significant differences between the evaluated tooth regions. As shown in Table 1, the second molar presented a higher prevalence of the more pronounced concavity subtypes, U-III (132 cases) and U-II (79 cases), whereas there was a predominance of types P (81 cases), U-I (63 cases), and C (43 cases) in the second premolar. The chi-square test showed a significant association between the cortical type and the tooth region ($p < 0.001$), confirming morphological differences between the 2PM and 2M.

No statistically significant differences were observed in the distribution of cortical types between sexes ($p = 0.166$) or between mandibular sides ($p = 0.564$). The right side showed a slight predominance of types U-III and U-II (81 and 58 cases, respectively), while the left side showed a similar distribution, with 68 cases of U-III and a higher concentration of U-II (69 cases). In the intra-tooth analysis between the mandibular sides, no statistically significant differences were observed in the distribution of the morphological types of the lingual cortex (C, P, and U) for both the mandibular second premolar ($p= 0.627$) and the mandibular second molar ($p > 0.05$).

Regarding the measurement variables between the right and left sides (Table 2), there was a significant difference for the vertical position of Point A (Vc) ($p < 0.001$). The Vc measurement presented lower values ($p < 0.001$) on the left side, indicating a more superior positioning of the point of greatest concavity prominence on this side. The variables D, Vb, Va, concavity angulation (β), WA, and WB did not show significant differences between sides ($p > 0.05$). In the intra-tooth analysis of the 2PM region, again only the Vc variable showed a significant difference between sides ($p = 0.004$) (Table 7). In contrast, in the mandibular second molar, significant differences were observed between sides for D ($p = 0.048$), Vc ($p = 0.016$), buccolingual width WA ($p = 0.004$), and buccolingual width WB ($p = 0.045$), with higher values on the right side (Table 8).

In Tables 3 and 4, no significant differences were identified between males and females for the variables D and concavity angulation (β) ($p > 0.05$). However, significant differences were identified for the variables Vb, Vc, Va, and for the buccolingual widths WA and WB ($p < 0.001$), indicating larger mandibular linear dimensions in males, without changes in the shape of the internal region of the concavity.

The most significant differences were observed between the second premolar and second molar regions. As shown in Tables 5 and 6, the second molar presented greater concavity depth ($p < 0.001$), greater angulation ($p < 0.001$), a more superior position of Point A ($p < 0.001$), and greater buccolingual widths WA and WB ($p < 0.001$). Furthermore, the Va measurement was significantly smaller in the

second molar (p = 0.002). Conversely, the second premolar presented shallower concavities, smaller angulation, and greater bone height availability.

5. Discussion

The posterior region of the mandible is an area of high surgical risk due to the presence of noble anatomical structures, such as the inferior alveolar nerve, the lingual nerve, and larger-caliber arteries [15]. In this context, the submandibular fossa plays a major role as it influences bone availability and presents morphological variations, several of which have already been described in the literature [1, 2, 3, 7, 13, 16]. However, its individual characteristics according to population, dental region, and sex remain poorly documented [18]. For its adequate assessment, cone-beam computed tomography (CBCT) is essential, enabling a three-dimensional analysis of this structure [1, 6, 7].

In the present study, approximately 73% of the evaluated regions exhibited a lingual concavity, a value comparable to those reported by Chan et al. (2010) [6] (66%) and Parnia et al. (2010) [1] (80%). A high prevalence of U-type lingual concavities was observed, with a predominance of the U-II and U-III subtypes, which accounted for 54.8% of the evaluated regions. These occurred mainly in the mandibular second molar, whereas the second premolars showed a higher frequency of P-type corticals and shallow U-I concavities. No statistically significant differences were found between the presence of concavity and sex (p = 0.1666), side (p = 0.564) or dental region a finding similar to that of Kamburoğlu et al. (2015) [8] regarding sex (p = 0.574). Nickenig et al. (2015) [12] also observed a concavity prevalence of approximately 68% across regions, which was higher in molars, particularly the second molar (2M).

The high frequency of moderate and deep concavities is explained by the anatomy of the submandibular fossa, given that its depth tends to increase progressively toward the posterior region of the mandible. Sadik et al. (2025) [7] observed a depth ≥ 2 mm in approximately half of their sample, a finding similar to our study, in which 53.17% of the regions presented a depth greater than 2 mm. Similar results were described by Sumer et al. (2015) (45%) [44] and Parnia et al. (2010) [1], who observed this condition in about 80% of the evaluated individuals. Depths equal to or greater than 2 mm are associated with a higher risk of lingual cortical perforation, severe hemorrhage, and compromise of the vascular structures of the floor of the mouth, especially during implant placement, periodontal surgeries, and complex extractions, as demonstrated by Mukherjee et al. (2025) [15] and Sun et al. (2022) [19].

Relevant morphometric differences were identified among the dental regions. The second premolar (2PM) showed greater available bone height (Va, p = 0.002) and more parallel ridges, whereas the 2M presented deeper concavities, greater angulation, and higher values for D, Vc, Wa, and Wb. This indicates a more superior position of the submandibular fossa, yet with smaller vertical ridges, resulting in closer proximity to the mandibular canal. Other studies have identified the 2M as the region of highest risk for lingual perforation [9, 12, 13, 20], whereas premolars tend to exhibit a flatter or more convex morphology [1, 6].

The distance between the alveolar crest and the lingual prominence of the concavity influences the implant trajectory and the available bone thickness, which may lead implants to bypass bone boundaries. Lower Vc values were observed in the left second premolar ($p = 0.004$). These findings reinforce that panoramic radiography is insufficient for assessing surgical risk, making CBCT indispensable for analyzing the depth and three-dimensional localization of the concavity [4, 11].

Although alveolar bone height is widely used as the primary criterion for selecting dental implant length, relying solely on its analysis can be a risk factor in the presence of deep concavities. In this study, the linear measurements Vb, Vc, Va, Wa, and Wb were significantly higher in male subjects ($p < 0.001$), corroborating the findings of Watanabe et al. (2010) [5], Mukherjee et al. (2025) [15], and Sadik et al. (2025) [7]. However, no significant differences were found between sexes regarding depth (D) or concavity angle, indicating that sexual dimorphism is related to bone volume rather than the shape of the concavity. Chan et al. (2010) [6] also observed no difference in depth between sexes (2.4 mm; $p = 0.99$), but reported a greater buccolingual width in men (7.8 mm) compared to women (6.9 mm; $p = 0.03$). This finding is similar to those of Ebrahimnejad et al. (2020) [2], Ijaz et al. (2020) [4], and Watanabe et al. (2010) [5]. Conversely, Alqutaibi et al. (2024) [13] found higher measurements in women across several parameters, while Kamburoğlu et al. (2015) [8] and Herranz-Aparicio et al. (2016) [20] found no correlation between measurements and sex, which may be attributed to ethnic differences, sample size, and variations in linear measurements. Thus, despite the larger mandibular volume in males, the anatomical risk of lingual cortical perforation is similar between sexes, since the "architecture" of the concavity remains constant [5, 13].

In addition to height, bone width proved to be a determining factor for surgical safety. The D, Vc, and Wa measurements showed higher values in the right second molar, indicating deeper and more inferior concavities. Although the superior buccolingual width (Wa) was greater on the right side (12.26 mm) compared to the left side (11.36 mm), this increase does not eliminate the risk of perforation, as greater bone thickness may coexist with an unfavorable internal configuration. Sun et al. (2022) [19] demonstrated that concavity depth and its angulation are the main determinants of implant distance to the lingual cortical plate, indicating that mandibular symmetry should not always be assumed, especially in the 2M region.

The literature presents conflicting results regarding lingual concavity and mandibular side. Sadik et al. (2015) [7] observed a mean depth of 1.98 ± 0.67 mm on the right side and 1.93 ± 0.65 mm on the left, while Alqutaibi et al. (2024) [13] also identified deeper concavities in the right second molar. Conversely, Tan et al. (2021) [21] reported values of 2.0 ± 0.6 mm on the right and 2.2 ± 0.6 mm on the left, and Bayrak et al. (2018) [22] found depths of 2.95 ± 0.84 mm e 2.85 ± 0.80 mm, respectively. Levingston (2025) [10] observed greater depth on the left side in a young population. Similarly, Sadik (2025) [7] identified a statistically significant difference between mandibular sides ($p = 0.001$), showing that this asymmetry may vary according to population, ethnicity, and functional characteristics. Sun et al. (2022) [19] described that the 2M, with a low and oblique quadrilateral morphology, is more prone to lingual

concavity than premolars, justifying the lower bone height (Va) and greater buccolingual widths (Wa and Wb).

Although the literature reports a low frequency of surgical accidents in the posterior mandible [7, 20, 23, 24], it is believed that cases of lingual cortical plate perforation are underreported, as they do not always result in immediate hemorrhage [3, 12]. Virtual simulation studies show that the incidence of lingual cortical perforation ranges between 1.1% and 1.2%, but can reach up to 22.2% in the 2M when larger diameter implants are used in Type-U ridges [3, 19]. Other studies report a probability of perforation varying between 0.8% and 31%, depending on the methodology and the population evaluated [7, 12, 23].

These data carry high clinical relevance, as demonstrated by several life-threatening hemorrhage reports, such as those described by Berberi et al. (1993) [25] and Givol et al. (2000) [26], in which perforation of the lingual plate resulted in acute airway obstruction and emergency interventions such as tracheostomy [1, 3, 9, 12, 8]. Other authors have also documented bleeding episodes following endosseous implant placement [25, 27]. The study by Isaacson et al. (2004) [28] described sublingual hematoma formation during the placement of mandibular endosseous implants as a rare but fatal complication, while Dubois et al. (2009) [29] reported two clinical cases of bleeding in the floor of the mouth resulting in respiratory failure due to upper airway obstruction. These were associated with injury to the sublingual, submental, or mylohyoid arteries arising from lingual cortical perforation [6, 7, 11]. Furthermore, perforations above the mylohyoid line can cause irreversible damage to the lingual nerve, while inferior perforations may allow the spread of infections into the parapharyngeal and retropharyngeal spaces [6, 7, 12]. In this context, an interdisciplinary approach is critical in managing surgical risks, where the identification of medications such as anticoagulants and bisphosphonates is known to compromise bone healing. In cases where larger-caliber arteries are severed, medical team collaboration is essential for imaging exams, emergency tracheostomy, and intra- and postoperative monitoring. These integrated protocols ensure better treatment predictability and patient safety [19, 30].

The morphological and morphometric variations of the submandibular fossa demonstrate differences in surgical risk among patients and reinforce the need for individualized three-dimensional evaluation, given that this structure does not present a single anatomical pattern. In this regard, the present study has limitations, such as the exclusive analysis of dentate individuals from a specific population. Consequently, the inclusion of both dentate and edentulous patients, alongside the correlation of anatomical findings with clinical outcomes in future studies, is necessary to expand the applicability and relevance of these results.

6. Conclusion

It is concluded that there is a high prevalence of lingual concavities in the posterior mandible, with a predominance of the U-II and U-III subtypes, particularly in the region of the mandibular second molars. This region is associated with a higher surgical risk due to greater concavity depth and angulation, as well as reduced vertical bone availability. Although male subjects exhibited larger bone dimensions, the

overall morphology of the submandibular fossa did not differ between sexes, indicating a similar anatomical risk. Furthermore, a greater extent of the concavities was observed on the right side, demonstrating a lack of mandibular symmetry. Consequently, a three-dimensional evaluation via cone-beam computed tomography is essential for safe surgical planning and the prevention of complications.

Declarations

Conflict of interest statement

The authors declare no conflicts of interest.

Compliance with Ethical Standards

Research involving Human Participants and/or Animals: Not applicable.

Informed consent: Not applicable.

Ethical Approval: The study was approved by the Permanent Ethics Committee on Research Involving Human Beings of the State University of Ponta Grossa (UEPG), Brazil. (CAEE: 69086823.3.0000.0105).

8. Author Contributions

J: Conceptualization, Methodology, Data Curation, Writing Original Draft.

A: Visualization (Tables and Figures).

F: Data Curation, Formal Analysis.

G: Conceptualization, Methodology, Writing – Review & Editing, Supervision.

K: Writing – Original Draft (Translation).

M: Conceptualization, Methodology, Writing – Review & Editing.

References

1. Parnia F, Fard EM, Mahboub F, Hafezeqoran A, Mojaver YH. Tomographic volume evaluation of submandibular fossa in patients requiring dental implants. Oral Surg Oral Med Oral Pathol Oral Radiol Endod. 2010;109(1):e32-e36.
2. Ebrahimnejad H, Sakhdari S, Soltani P, et al. Evaluation of mandibular lingual concavity in premolar and molar region using cone-beam computed tomography (CBCT). J Kerman Univ Med Sci. 2022;29(1):24–30.
3. Chan HL, Wang HL, Fenech M, et al. Cross-sectional analysis of the mandibular lingual concavity using cone beam computed tomography. Clin Oral Implants Res. 2011;22(2):201-206.

4. Ijaz M, Shahzad MA, Ahmed S, et al. Evaluation of Mandibular Ridge Lingual Concavity Using Cone Beam Computed Tomography. J Bahria Univ Med Dent Coll. 2020;10(4):306-311.
5. Watanabe H, Goseki T, Namaki S, Radwan M, Ariji K, Ariji E. Mandible size and morphology determined with CT on a premise of dental implant operation. Surg Radiol Anat. 2010;32(4):343-349.
6. Chan HL, Brooks SL, J Z, Benavides E, Wang HL. Risk assessment of lingual plate perforation in posterior mandibular region: a virtual implant placement study using cone-beam computed tomography. J Periodontol. 2011;82(1):129-135.
7. Sadik E, Kilic E, Alkan A, et al. Evaluation of submandibular fossa depth and mandibular canal relationship with cone-beam computed tomography. BMC Oral Health. 2025;25(1):601.
8. Kamburoğlu K, Kılıç C, Özen T, Horasan S. CBCT quantitative evaluation of mandibular lingual concavities in dental implant patients. Surg Radiol Anat. 2015;37(10):1209-1215.
9. Uchida Y, Yamashita Y, Goto M, Hanihara T, Takahashi H. Anatomic measurement of the depth and location of the sublingual fossa. Int J Oral Maxillofac Surg. 2012;41(12):1571-1576.
10. Levingston S, et al. Assessment of the submandibular fossa depth and diameter of the mandibular canal via cone beam computed tomography: a comparative study. Maxillofac Plast Reconstr Surg. 2025;47(1):19.
11. Özeren Keşkek C, Aytuğar E. Factors influencing submandibular fossa visibility on panoramic images: a comparative CBCT study. BMC Oral Health. 2024;24(1):1556.
12. Nickenig HJ, Eitner S. Reliability of implant placement after virtual planning of implant positions using cone beam CT data and surgical (guide) templates. J Craniomaxillofac Surg. 2007;35(4-5):207-211.
13. Alqutaibi AY, et al. Quantitative and qualitative 3D analysis of mandibular lingual concavities: implications for dental implant planning in the posterior mandible. Clin Exp Dent Res. 2024;10(1):e858.
14. Rajput BS, et al. Assessment of lingual concavities in submandibular fossa region in patients requiring dental implants: a cone beam computed tomography study. J Contemp Dent Pract. 2018;19(11):1329-1333.
15. Mukherjee S, et al. Proposed Classification System for Submandibular Gland Fossa Anatomy and Its Radiomorphometric Assessment Using Cone-Beam Computed Tomography: A Retrospective Study. Cureus. 2025;17(1):e77301.
16. Şahan HT, Doğan ME, Görgün EA. Retrospective Evaluation of Submandibular Fossa Depth in Relation to Mandibular Canal and Bone Thickness: CBCT-based Study. Curr Med Imaging. 2025;21(1):e15734056386043.
17. Tal H, Moses O. A comparison of panoramic radiography with computed tomography in the planning of implant surgery. Dentomaxillofac Radiol. 1991;20(1):40-42.
18. Leong DJM, et al. Risk of lingual plate perforation during implant placement in the posterior mandible: a human cadaver study. Implant Dent. 2011;20(5):360-363.

19. Sun Y, et al. Relevant factors of posterior mandible lingual plate perforation during immediate implant placement: a virtual implant placement study using CBCT. BMC Oral Health. 2023;23(1):76.
20. Herranz-Aparicio J, et al. Retrospective study of the bone morphology in the posterior mandibular region: evaluation of the prevalence and the degree of lingual concavity and their possible complications. Med Oral Patol Oral Cir Bucal. 2016;21(6):e731-e736.
21. Tan WY, et al. Evaluation of anatomic variations of mandibular lingual concavities from cone beam computed tomography scans in a Malaysian population. J Prosthet Dent. 2021;125(6):766.e1-766.e8
22. Bayrak S, et al. Correlation between the visibility of submandibular fossa and mandibular canal cortication on panoramic radiographs and submandibular fossa depth on CBCT. Med Oral Patol Oral Cir Bucal. 2018;23(1):e105-e111.
23. Huang RY, et al. Risk of lingual plate perforation for virtual immediate implant placement in the posterior mandible: a computer simulation study. J Am Dent Assoc. 2015;146(10):735-742.
24. Alzaben B, et al. The prevalence of mandibular lingual concavity among the Saudi population of Eastern Province: A CBCT evaluation. Saudi Dent J. 2024;36(8):1618-1622.
25. Berberi A, et al. Lingual paresthesia following surgical placement of implants: report of a case. Int J Oral Maxillofac Implants. 1993;8(5):580-582.
26. Givol N, et al. Emergency tracheostomy following life-threatening hemorrhage in the floor of the mouth during immediate implant placement in the mandibular canine region. Journal of Periodontology. 2000;71(12):1893-1895.
27. Laboda G. Life-threatening hemorrhage after placement of an endosseous implant: report of case. J Am Dent Assoc. 1990;121(5):599-600.
28. Isaacson TJ. Sublingual hematoma formation during immediate placement of mandibular endosseous implants. J Am Dent Assoc. 2004;135(2):168-172.
29. Dubois L, et al. Excessive bleeding in the floor of the mouth after endosseus implant placement: a report of two cases. Int J Oral Maxillofac Surg. 2010;39(4):412-415.
30. Asa ME, Serpe L. Immediate complications in the surgical phase associated with implant dentistry: causes and management. Lumen et Virtus. 2025;16(48):5635-5660.

Tables

Tables 1 to 8 are available in the supplementary files section

Graph 1

Graph 1 is available in the Supplementary Files section.

Figures

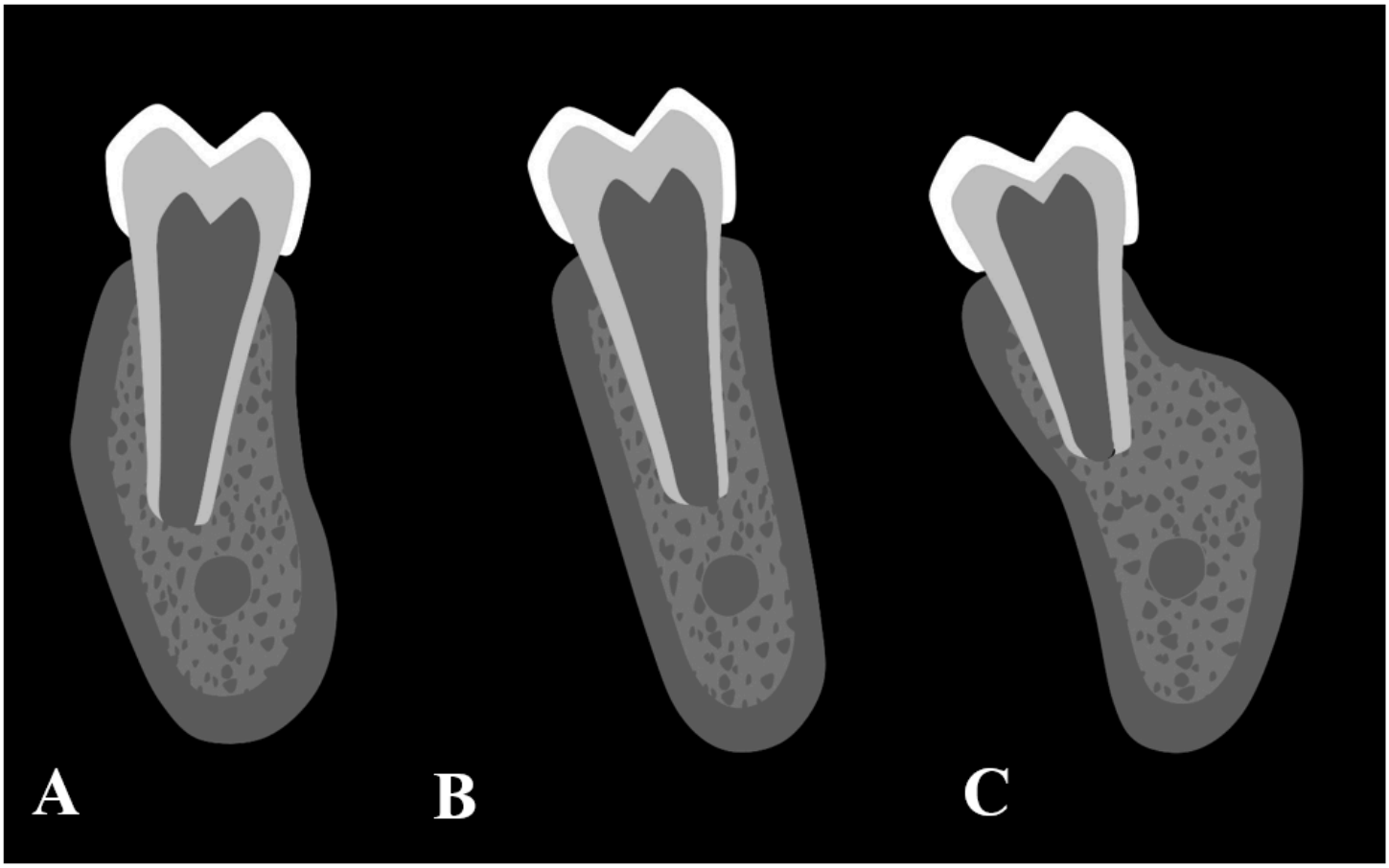


Figure 1

Schematic representation of the mandibular lingual cortex morphological types: (A) Convex type, (B) Parallel type, and (C) Concave/Undercut type.

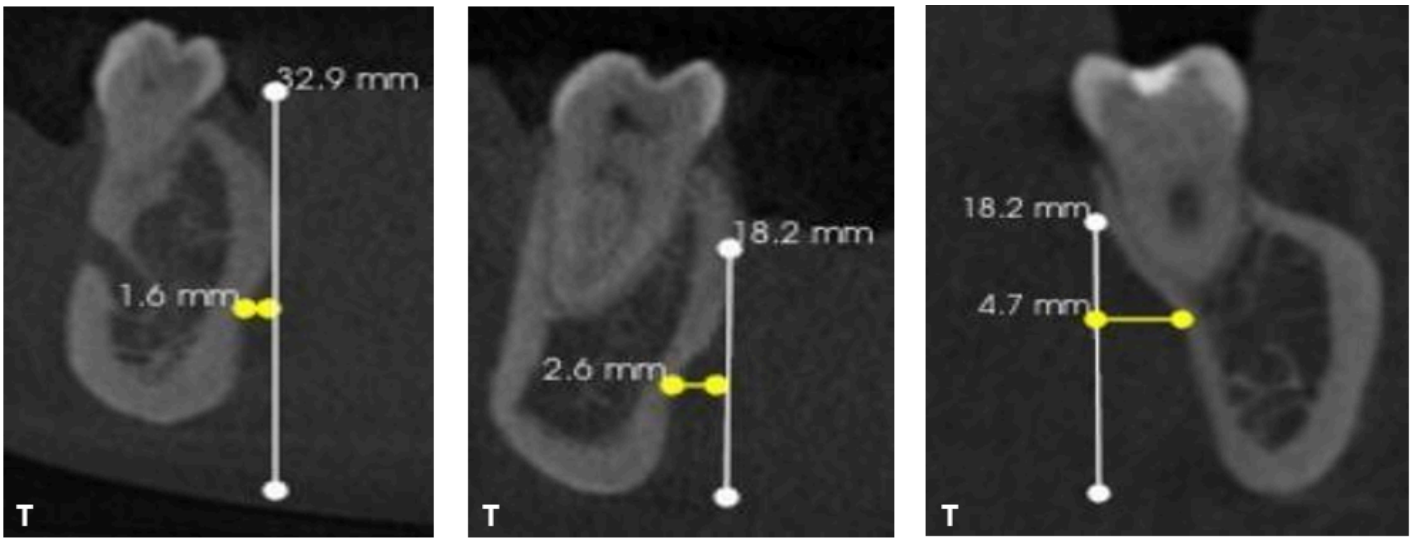


Figure 2

Morphological classification of the "U-type" mandibular lingual cortex: Type I, Type II, and Type III.

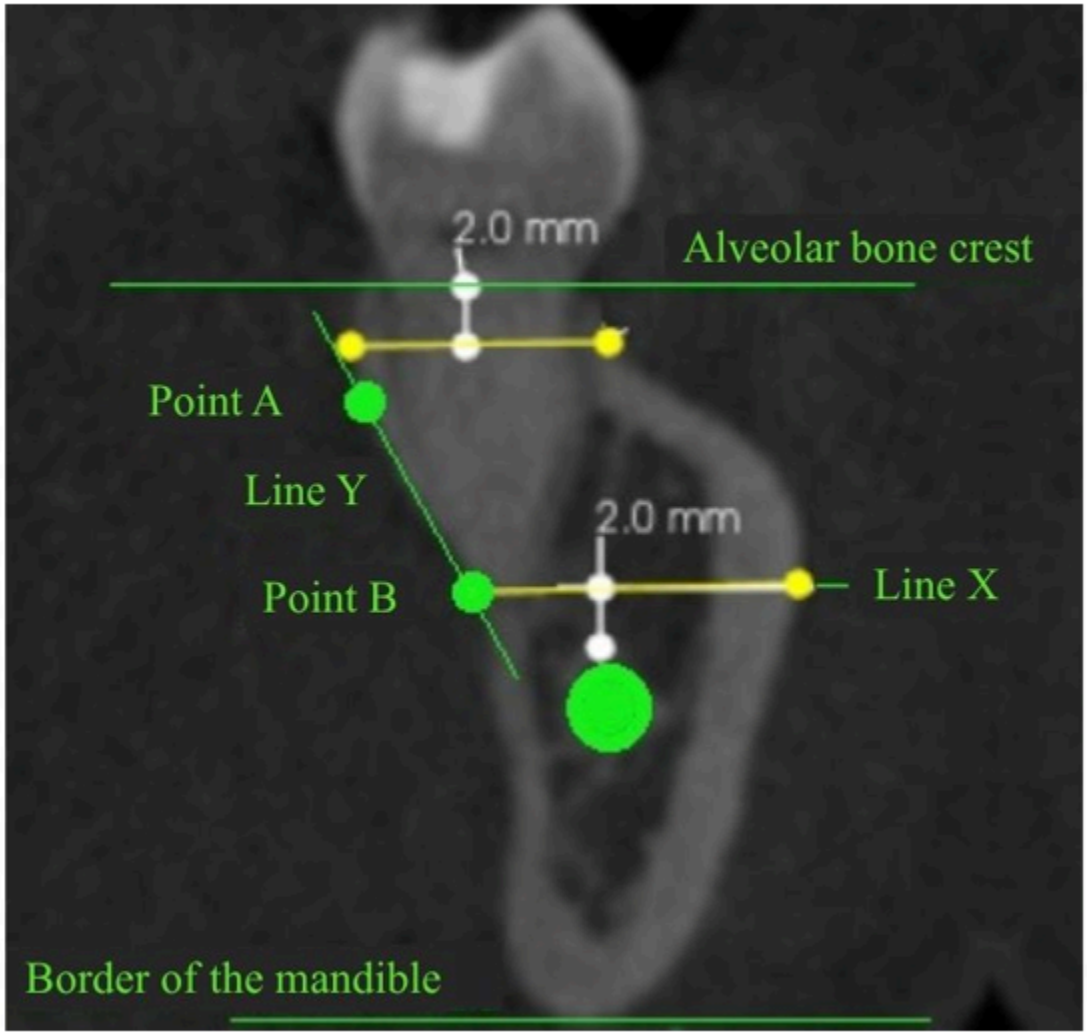


Figure 3

Tomographic aspect of the mandible in the second molar region, showing the alveolar bone crest, Line X (2mm above the mandibular canal), Line Y (formed from Point A towards Line X), Point A (lingual prominence), Point B (intersection of Line X with the lingual cortex), the 2mm reference below the alveolar bone crest and above the inferior border of the mandible, and the MC.

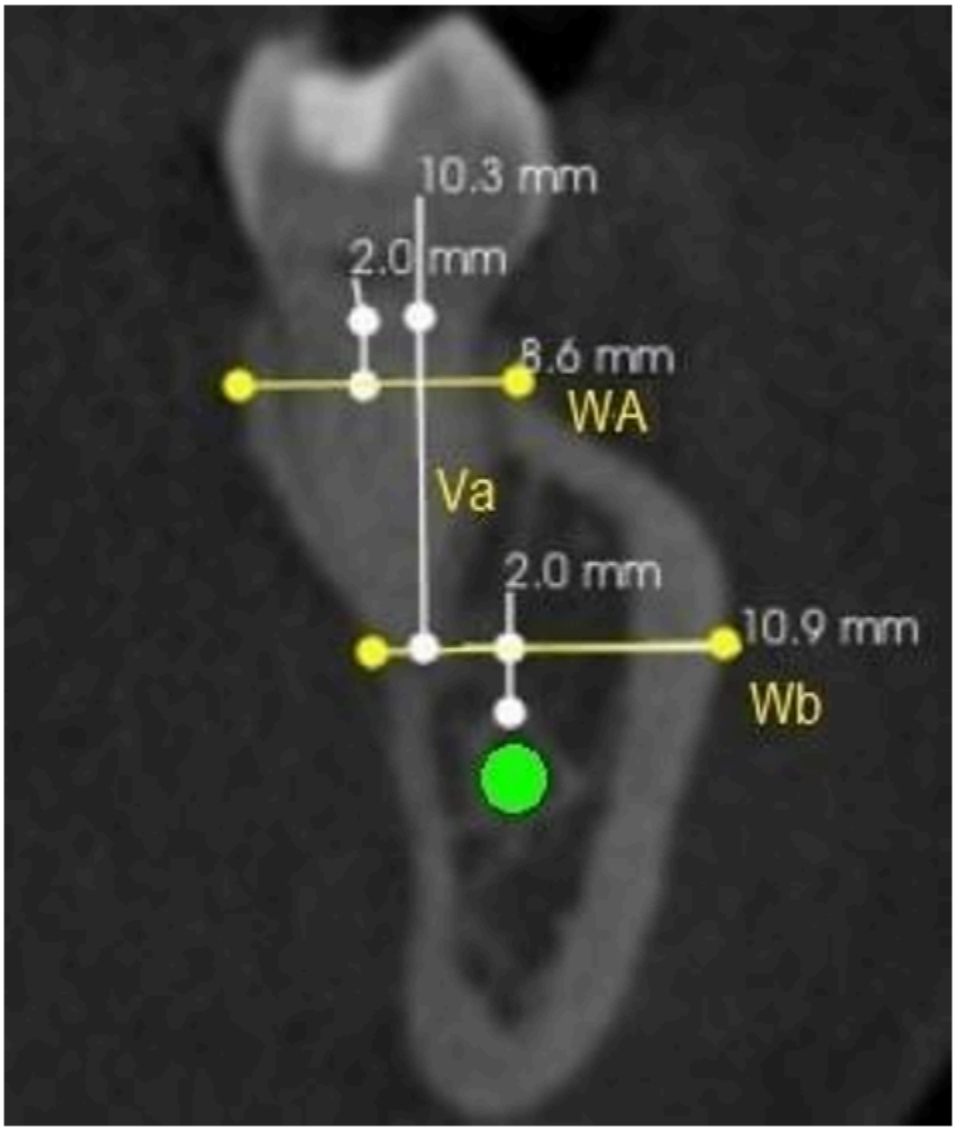


Figure 4

Adjusted cross-section of the mandible in the second molar region, illustrating the measurements: WA (crest width 2mm below the alveolar level), VA (vertical distance between the alveolar crest and reference Line X), and WB (crest width 2 above the MC level).

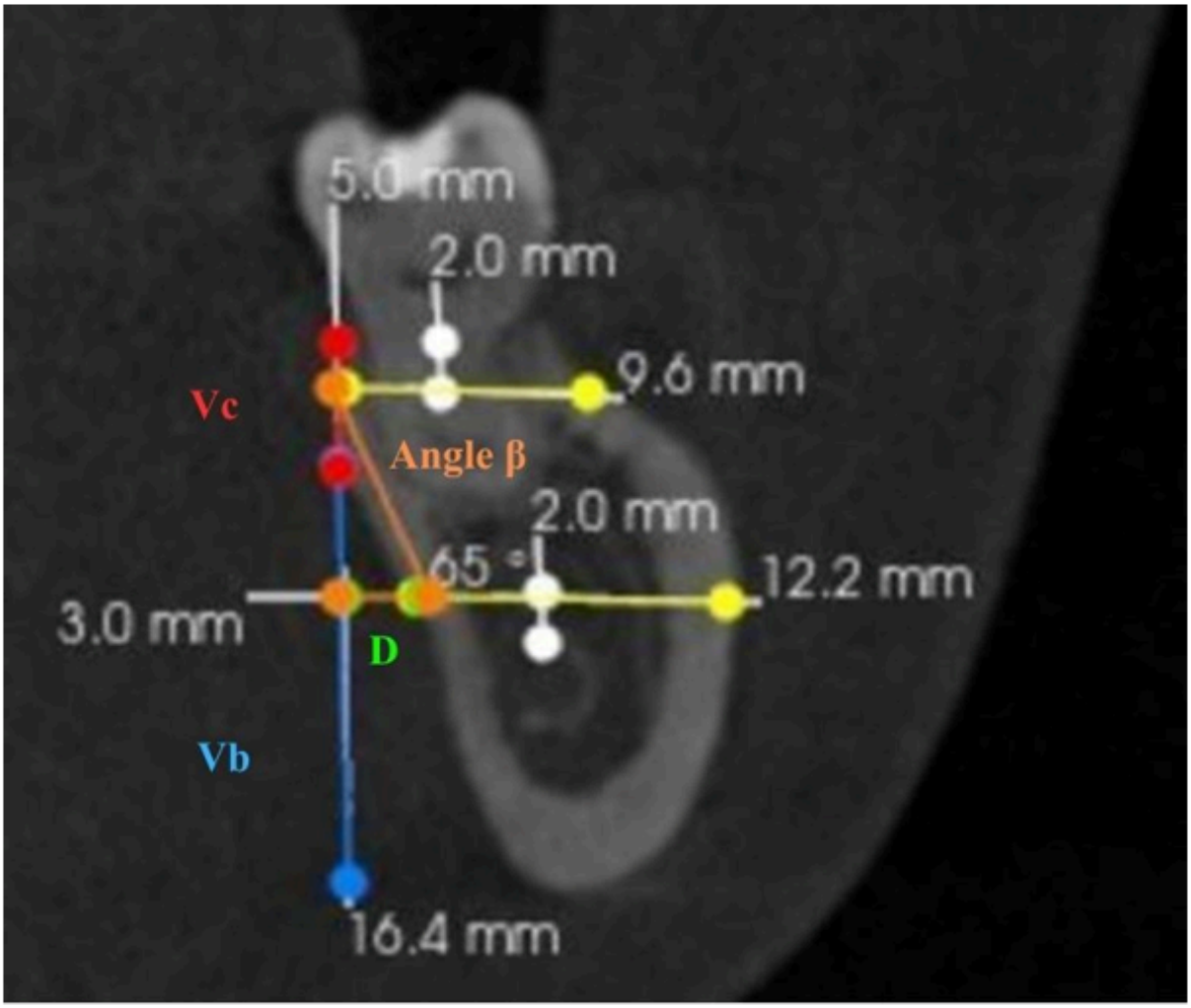


Figure 5

Adjusted cross-section of the mandible in the second molar region, demonstrating the measurements: Vc (vertical distance from the crest to Point A), Angle β (lingual concavity angle), D (linear depth of the concavity), and Vb (vertical distance).

Supplementary Files

This is a list of supplementary files associated with this preprint. Click to download.

- Tables.docx
- Graph1.docx